ISIEA 2010

2010 IEEE Symposium on Industrial Electronics & Applications

Incorporating Colloquium on Humanities, Science and Engineering Research (CHUSER 2010)

Sponsors:

IEEE Advancing Technology for Humanity

pels

ies

IAS IEEE INDUSTRY APPLICATIONS SOCIETY

IEEE Malaysia PEL/IE/IA Joint Chapter

Co-organiser:

Universiti Teknologi MARA

Research Management Institute RMI

3 - 5 October 2010
Park Royal Penang Hotel
Malaysia

www.mypels.org/mypels

PROGRAM AND ABSTRACTS

ISIEA 2010

PROGRAM & ABSTRACT

Park Royal Hotel, Penang
3-5 October 2010

CONTENTS

WELCOME MESSAGE

On behalf of the Organizing Committee of the IEEE Symposium on Industrial Electronics and Applications (ISIEA2010), it gives me great pleasure in welcoming all delegates to Penang, Malaysia. ISIEA2010 is held from 3 to 5 October 2010 at the Park Royal Hotel, Penang, Malaysia. The event also incorporates the Colloquium on Humanities, Science and Engineering Research (CHUSER 2010). The event is sponsored by the IEEE Malaysia, the IEEE Malaysia Power Electronics (PEL)/Industrial Electronics(IE)/ Industrial Applications (IA) Joint Chapter and co-organised with the Research Management Institute of UiTM.

The purpose of the symposium is to create a forum for scientists, engineers and practitioners throughout the world to present the latest techniques in Industrial Electronics and its associated applications. In line with IEEE's vision of Advancing Technology for Humanities beyond traditional boundaries, a track on Humanities and Commercial applications has been introduced.

We very glad to mention that the Proceedings of ISIEA 2010 will be included in the IEEE Xplore database.

We have received overwhelming response with a total of 289 full paper submissions from 36 different countries. Our 435 reviewers worldwide selected papers through a rigorous review process of which finally 137 papers are to be presented at the event.

On behalf of the organizing committee we would like to take this opportunity to express our gratitude to all reviewers who have been working hard to finish reviews on time and hence ensured the success of this event. Members of the International Advisory Committee deserve special appreciation as they played key supportive role in the symposium organization. We would like to thank all authors, session chairpersons, reviewers and delegates for your great support and contribution to ISIEA2010. Last but not least are the Organizing Committee, colleagues and friends who have been working behind-the-scenes; who deserve special mention. Without their unfailing cooperation, hard work and dedication, this event would simply not be possible.

The technical program starts on the afternoon of 3 October 2010 (Sunday) with 3 tutorial sessions conducted by leading experts. A welcome reception is planned for Sunday evening and a Gala Dinner on Monday evening. Throughout these events, we hope to create an opportunity for old friends and colleagues to get together, and more importantly, to become new peers in diverse areas of expertise. The event is scheduled with 12 oral sessions with 3 sessions running in parallel at a time.

I understand that many delegates are here in Malaysia for the first time. I would like to encourage you to explore the beautiful sights of Malaysia during your stay and do enjoy the symposium.

MUSTAFAR KAMAL HAMZAH
General Chair, ISIEA2010

MOHD KHAIRUL MOHD SALLEH
Technical Program Chair, ISIEA2010

ORGANIZING COMMITTEE

General Chair:
Mustafar Kamal Hamzah

Organising Co-Chair:
Mohd Nasir Taib

Secretary:
Nor Farahaida Abdul Rahman

Finance Chair:
Siti Zaliha Mohammad Noor

Exhibition/Sponsorship Chair :
Gobbi Ramasamy

Publication Chair :
Mohd Nawawi Seroji

Local Arrangement Chair I :
Noorsalissa Saedan

Local Arrangement Chair II :
Mohd Faizul Idros

Publicity Chair & Webmaster :
Ihsan Mohd Yassin

Steering Committee
Mustafar Kamal Hamzah(Chair)
Wahidah Mansor (EMB)
Ahmad Sabirin Zoolfakar (UiTM SB)
Ngah Ramzi Hamzah (IM)
Gobbi Ramasamy (PEL/IE/IA)
Mohd Nawawi Seroji (PEL/IE/IA)
Mohd Rezal Mohamed (PEL/IE/IA)
Zuhaina Zakaria (WIE)

Technical Program Committee

Technical Program Chair:
Mohd Khairul Mohd Salleh, Universiti Teknologi MARA

Track Chairs :
Makbul Anwari, Universiti Teknologi Malaysia
Nik Rumzi Nik Idris, Universiti Teknologi Malaysia
Gobbi Ramasamy, Multimedia Universiti
Azilah Saparon, Universiti Teknologi MARA
Nooritawati Md Tahir, Universiti Teknologi MARA
Kamal Zuhairi Zamli, Universiti Sains Malaysia
Habibah Hashim, Universiti Teknologi MARA
Rini Akmeliawati, International Islamic University
Ngah Ramzi Hamzah, Universiti Teknologi MARA
Wahidah Mansor, Universiti Teknologi MARA
Fatimah Ibrahim, Universiti Malaya
Mohd Rizal Arshad, Universiti Sains Malaysia
Normah Omar, Universiti Teknologi MARA
Rozainun Abdul Aziz, Universiti Teknologi MARA
Mohd Juzaiddin Ab Aziz, Universiti Kebangsaan Malaysia
Abdul Manan Abdul Samad, Universiti Teknologi MARA

INTERNATIONAL ADVISORY/LIASON

Okyay Kaynak
Bogazici Univ, Turkey

Dean Patterson
University of Nebraska-Lincoln, USA

Dushan Boroyevich
Virginia Tech, USA

Abdul Halim Mohd Yatim
Universiti Teknologi Malaysia

Norman Mariun
Universiti Putra Malaysia

Subhas Mukhopadhyay
Massey University, New Zealand

Abu Bakar Majeed
Universiti Teknologi MARA

Gourab Sen Gupta
Massey University, New Zealand

Toshio Fukuda
Nagoya University, Japan

Bhim Singh
Indian Institute of Technology, India

Andrew Forsyth
University of Manchester, United Kingdom

Serge Demidenko
Monash University, Malaysia

REVIEWERS

Abd Kadir Mahamad
Abdelbaset Khalaf
Abdul Ali
Abdul Halim Yatim
Abdul Jaleel Jalaludeen
Abdullahi Arabo
Abdulwahid Al-Saif
Abolfazl Jalilvand
Ahmad Asari Sulaiman
Ahmad Fauzi Abas
Ahmad Sabirin Zoolfakar
Ahmed Zeki
Ahmed Zobaa
Aini Hussain
Akhtar Ali Jalbani
Aladin Zayegh
Alicia Tang Yee Chong
Alie El-Din Mady
Alireza Rezvanian
Al-Khalid Othman
Amad Mourad
Amidedin Mousavi
Amir Shah Abdul Aziz
Aneel Rahim
Anees Abdul Aziz
Angkoon Phinyomark
Anis Nordin
Ankit Salgia
Anna Cysewska-Sobusiak
Anton Satria Prabuwono
Arshin Rezazadeh
Arturo Rodriguez
Ashab Mirza
Asish Mukhopadhyay
Atul Negi
Azian Azamimi Abdullah
Azilah Saparon
Azran Azhim
Azwan Abdul Rashid
Badrul Hisham Ahmad
Balza Achmad
Bashar Tahayna
Bee Ee Khoo
Bendaoud Abdelber
Biju Issac
Boto Bako
Carlos Gutierrez
Cheng-Ta Chiang
Chi-Ming Wong
Chitti Babu B
CMR Prabhu
Dae Gun Lee
Dahaman Ishak
Dakshina Ranjan Kisku
Danish IRFAN
Darwin Jose Raju
David Brown
Deepak Yadav
Demian D'Mello
Dinesh Sathyamoorthy
Dirman Hanafi
Don Dissanayake
Duduku V Viswacheda
Eduard Babulak
Eduardo Pinheiro
Ekachai Leelarasmee
El-Sayed Hasaneen
Emilio JimÃ©nez MacÃ-as
Farshad Fahimi
Farzad Tahami
Fathima Rawoof
Fen Zhou
Francisco Torrens
GaÃ«tan Prigent
Gerino Mappatao
Ghafour Amouzad Mahdiraji
Gnana Joseph
Gobbi Ramasamy
Gordana Jovanovic Dolecek
Gourab Sen Gupta
Guruprasad Hegde
Haikal El Abed
Hajar Mat Jani
Hamid Nooralizadeh
Hamidah Ibrahim
Hamzah Ahmad
Hanny Tumbelaka
Hasnida Saad
Hazry Desa
Hedi Harizi
Hengky Susanto
Henry Yuk-tung Ngan
Herdawatie Abdul Kadir
Herlina Abdul Rahim
Himanshu Agrawal
Hu Jintao
Hua Nong Ting
Hung-Liang Cheng
Husna Abdul Rahman
Husna Zainol Abidin
Hussain Al Abdulqader
Hyunglae Lee
Ihsan Yassin
Intan Rahayu Ibrahim
Iwan Adhicandra
Jaeho Choi
Jamilah Karim
Jerzy Domzal
Jianwu Xu
JoaquÃ-n Olivares Bueno
JosÃ© Silva
Juan JosÃ© GonzÃ¡lez de la Rosa
Juliana KnocikovÃ¡
Junyong You
Kaharudin Dimyati
Kamal Zuhairi Zamli
Kamel Tourki
Kamil Dimililer
Kaouthar Benameur
Karim Ouertani
Karthikeyan Rajagopal
Kartik Prasad Basu
Kenneth Sundaraj
Khairuddin Mohammad
Khairulmizam Samsudin
Khaled Hamdan
Khaled Suwais
Khine Nyunt
Kittipong Tripetch
Krishna Battula
Krishnanand Kaipa
Lakhoua Mohamed Najeh
Lefteris Angelis
Lei Jiao
Lei Ma
Linda Mohd Kassim
Lokman
M Ayoub Khan
M. Hadi Mashinchi
Madjid Khalilian
Majid Delshad
Majid Haghparast
Makbul Anwari
Makhfudzah Mokhtar
Mandava Rajeswari
Manoj Datta
Manoj Sharma
Marius Branzila
Markus Pfeifer
Mas Izyani Md Ali
Mazidah Puteh
Md Ismail
Md. Mamun Bin Ibne Reaz
Md. Rajibul Islam
Media Ayu
Mehdi Bahrami
Mehdi EffatParvar
Messaouda Azzouzi
Michele Fiorini
Miftahur Rahman
Mohamad Hafiz Mamat
Mohamed Awad
Mohamed Dahidah
Mohammad Faridun Naim Tajuddin
Mohammad Hamiruce Marhaban
Mohammad Nawawi Seroji
Mohammad Reza Amini
Mohammad Reza Faieghi
Mohammad Zia Ur Rahman
Mohammed Al-Faiz
Mohammed Younis
Mohd Ariff Kasim
Mohd Ashraf Ahmad
Mohd Azri Abdul Aziz
Mohd Faiz Hilmi
Mohd Faizul Idros
Mohd Fareq Abd Malek
Mohd Juzaidin Ab Aziz
Mohd Khairul Mohd Salleh
Mohd Najib Mohd Hussain
Mohd Rezal
Mohd Rizal Arshad
Mohd. Hafiz Ismail

TECHNICAL PROGRAM OVERVIEW

Time	JINTAN	LAWANG	PALA
Sunday, October 3			
14:40	T11: *Tutorial 1*	T21: *Tutorial 2*	T31: *Tutorial 3*
15:40	*Afternoon Break 1*		
16:00	T12: *Tutorial 1 (cont)*	T22: *Tutorial 2 (cont)*	T32: *Tutorial 3 (cont)*
18:00	*WELCOMING EVENING COCKTAIL (BALLROOM)*		
Monday, October 4			
08:40	A11: *Power Electronics I*	B11: *Communications Technology I*	C11: *Instrumentation & Signal Processing*
10:40	*Morning Break 1 (Foyer)*		
11:00	A12: *Power Electronics I (cont)*	B12: *Communications Technology I (cont)*	C12: *Instrumentation & Signal Processing (cont)*
13:00	*Lunch Break (Hotel Cafe)*		
14:00	A21: *Power Electronics/Power Technologies*	B21: *Communications Technology II*	C21: *Humanities/Computer*
15:40	*Afternoon Break 2 (Foyer)*		
16:00	A22: *Power Electronics/Power Technologies (cont)*	B22: *Communications Technology II (cont)*	C22: *Humanities/Computer (cont)*
19:30	*PHOTO SESSION (Hotel Entrance in front of ISIEA2010 Banner)*		
20:00	*GALA DINNER (BALL ROOM)*		
Tuesday, October 5			
08:40	A31: *Biomedical & Bioinformatics*	B31: *Electronic Design I*	C31: *Power Engineering/Mechatronics*
10:40	*Morning Break 3 (Foyer)*		
11:00	A32: *Biomedical & Bioinformatics (cont)*	B32: *Electronic Design I (cont)*	C32: *Power Engineering/Mechatronics (cont)*
13:00	*Lunch Break 3 (Hotel Cafe)*		
14:00	A41: *Biomedical/Computation*	B41: *Electronic Design II*	C41: *Signal Processing*
15:40	*Afternoon Break 3 (Foyer)*		
16:00	A42: *Biomedical/Computation (cont)*	B42: *Electronic Design II (cont)*	C42: *Signal Processing (cont)*

2010 IEEE Symposium on Industrial Electronics and Applications (ISIEA 2010), October 3-5, 2010, Penang, Malaysia

Simple Integration of Three-phase Shunt Active Power Filter and Photovoltaic Generation System with Fibonacci-Search-Based MPPT

Hanny H. Tumbelaka
Department of Electrical Engineering
Petra Christian University
Surabaya, Indonesia
e-mail: tumbeh@petra.ac.id

Masafumi Miyatake
Department of Engineering and Applied Sciences
Sophia University
Tokyo, Japan
e-mail: miyatake@sophia.ac.jp

***Abstract* — This paper proposes a three-phase four wire current-controlled Voltage Source Inverter (CC-VSI) for both harmonic mitigation and PV energy extraction. For harmonic mitigation, the CC-VSI works as a grid current-controlling shunt active power filter. Then, the PV array is coupled to the DC bus of the CC-VSI. The MPPT controller employs the Fibonacci search method. The output of MPPT controller is a DC voltage that determines the DC-bus voltage according to the PV maximum power. From computer simulation, the CC-VSI can effectively compensate for harmonics as well as deliver PV power to the grid.**

***Keywordss* — Active Power Filter, MPPT, PV Energy Conversion.**

I. INTRODUCTION

In AC-DC power conversion, a DC side is generally connected to a DC load or, in many applications, a power source such as batteries and photovoltaic panels. On the other hand, an AC side is often an AC load or can be a voltage source from a power utility, or a generator.

In order to control the desired power flow between the DC side and the AC side, a high-frequency switched power converter is usually applied. The power converter (inverter) consists of power semiconductor switches with energy storage devices. The basic popular type of a power converter is a Voltage Source Inverter (VSI) because it is easy to implement, low loss and low cost. Nowadays, power flow control in the VSI (especially for grid connected system) can be achieved using a current-control technique. By controlling the switching instants, the current-controlled VSI (CC-VSI) produces the desired current flow using instantaneous current feedback [1].

A CC-VSI can be used as a shunt active power filter (APF) to improve the power quality of the power system [2-4]. The power converter operates to cancel the harmonics, as well as reactive power from the non-linear loads so that the grid currents will be sinusoidal with unity power factor. The AC side of the CC-VSI attaches to the AC grid at the point of common coupling (PCC) and parallel to the loads, while the DC bus of the CC-VSI contains a DC capacitor.

A CC-VSI can also be applied to transfer active power from a DC source to the AC grid (grid-connected system), as well as to the loads. The AC side of the CC-VSI attaches to the utility grid at the PCC, while the DC side of the CC-VSI is connected to a battery or a renewable energy source such as Photovoltaic system. If connected to solar cells, it is expected that the VSI has the ability to track the maximum power extracted from the PV panels. In literatures [5-7], the power converter operates as a single-stage circuit to achieve directly DC-AC energy transfer with maximum power point tracking (MPPT).

Since the CC-VSI for transferring active power and for canceling harmonics has a similar configuration, it is potential to integrate both functions in one CC-VSI. In this way, the power converter would be able to improve the system power quality as well as to deliver energy from renewable energy sources.

There are few literatures that discuss about combining PV power extraction and active filtering such as in [8-9]. Literature [8] requires calculation of load active power and PV output power to determine the inverter current. Due to switching device safety, power flow of PV power is processed first, while power quality improvement is in the second priority. Moreover, DC-bus controller is used during no insolation. In [9], the current controller requires the measurement of both the load and the inverter currents. The load current is used to calculate the reactive- and harmonic-rich reference value for the inverter current that could create errors and time delays.

This paper proposes a simple and reliable way to integrate active filtering and PV power extracting in one CC-VSI. In addition, the MPPT controller used in this paper is Fibonacci-search-based MPPT. The effectiveness of the MPPT controller and its compatibility with the CC-VSI controller will also be explained. By doing this, the energy efficiency of the system would be significantly increased.

II. THE CC-VSI

The three-phase four-wire CC-VSI for active filter and PV energy extraction is essentially three independent single-phase inverters with a common DC bus. There are inductors at the AC side and a mid-point earthed split capacitor at the DC-bus. It consists of a current control loop to control the harmonic and reactive power and a voltage control loop to control the active power [3-4]. The speed of response of the voltage control loop is much slower than that of the current control loop. Hence, the current control loop and voltage control loop are

978-1-4244-7646-6/10/$26.00

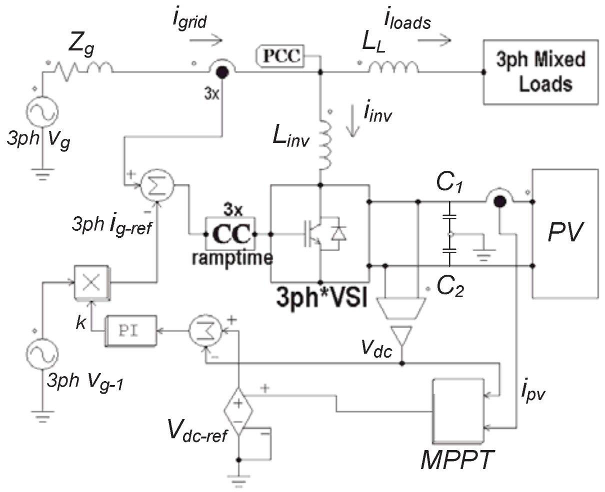

Figure 1. The proposed CC-VSI configuration

decoupled. Moreover, there is a PV array supported by a MPPT controller, which is coupled to the DC-bus of the CC-VSI. Fig. 1 shows the proposed CC-VSI configuration.

A. *Current Control Loop*

The current control loop shapes the grid currents, rather than VSI currents, to be sinusoidal and in-phase with the grid voltages by generating a certain pattern of bipolar PWM for continuous switching of the power converter switches according to a ramptime current control technique.

The ramptime current control (RCC) technique has been established as described in the literature [1][12][13]. The principle operation of RCC is similar to a sliding mode control and based on the concept of zero average current error (ZACE). The current error signal is forced to have an average value equal to zero with a constant switching frequency. The RCC maintains the area of positive current error signal excursions equal to the area of negative current error signal excursions, resulting in the average value of the current error signal being zero over a switching period (Fig. 2). The switching period (or frequency) is also kept constant based on the choice of switching instants relative to the zero crossing times of the current error signal. The RCC has a high bandwidth with a fast transient response that can quickly follow the rapid changes in non linear loads.

In this case, the current sensors are located on the grid side. The grid currents are sensed and directly controlled to follow symmetrical sinusoidal reference signals ($i_{g\text{-}ref}$), which is in-phase with the grid voltages. The reference signal waveform is the same as the fundamental component of the grid voltage, which is obtained using a phase-lock-loop (PLL) circuit. Hence, the outputs of the sensors are compared to the reference signals. The current error signals, which are the difference between the actual currents (grid currents – i_{grid}) and the reference signals – $i_{g\text{-}ref}$, are processed using ramptime current control to generate PWM signals for driving the power switches.

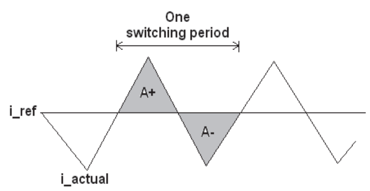

Figure 2. Zero average current error (ZACE)

Therefore, by forcing the grid currents to be identical to the reference signals, the CC-VSI operates as a shunt active power filter (APF) and automatically provides the harmonic, reactive, negative- and zero-sequence currents for the load according to the basic current summation rule (1) without measuring and determining the unwanted load current components.

$$i_{grid} = i_{inv} + i_{loads} \qquad (1)$$

B. *Voltage Control Loop*

The voltage control loop is a simple Proportional Integral (PI) control to keep the DC-bus voltage at the reference voltage level ($V_{dc\text{-}ref}$) and to provide the amplitude of grid currents. In the voltage control loop, the active power is maintained balanced among the grid, the load and the VSI.

If active power unbalance occurs in the system, there is a voltage deviation (ΔV_{dc}) in the DC bus relative to the reference voltage. For perfect tracking in the current control loop, the voltage control loop responds to adjust the amplitude of grid currents appropriately by adjusting the amplitude of $i_{g\text{-}ref}$ as well as to recover the DC-bus voltage to the reference voltage level. The output of the PI controller, which is a gain k, can determine the amount of ΔV_{dc} that corresponds to the grid current amplitude. The average DC-bus voltage is then recovered and stays at the reference voltage. New steady state active power balance has been achieved with new grid current amplitude. The sinusoidal grid current reference signal is given by

$$i_{g\text{-}ref} = k\, v_{g\text{-}1} \qquad (2)$$

where $v_{g\text{-}1}$ is the fundamental component of the grid voltage obtained from a PLL circuit. The value of k is the output of the PI controller. This is an effective way of determining the required magnitude of the grid current, since any mismatch between the required load active power and that being forced by the CC-VSI would result in the necessary corrections to regulate the DC-bus voltage.

III. PV ENERGY CONVERSION

The CC-VSI configuration in Fig. 1 has a capability to deliver the solar energy to the AC grid. PV arrays are coupled to the DC bus and parallel to DC-bus capacitors (C_1 and C_2). The amount of active power injected from PV panels is determined by the PV output voltage, which is equal to the DC bus voltage (v_{dc}). For PV array with 1 parallel string and 25 series modules per string, the *p-v* curve of Fuji Electric PV modules (ELR-615-160Z) for several levels of irradiance is shown in Fig. 3. The fluctuation of solar irradiation leads to the variation of PV output power.

The PV modules have to be arranged in an array such that the PV output voltage has to be greater than twice of the peak value of the grid voltage [10]. Otherwise, the CC-VSI is unstable and unable to deliver currents to the grid. On the other hand, there is an upper limit to satisfy voltage insulation requirements of power electronic components.

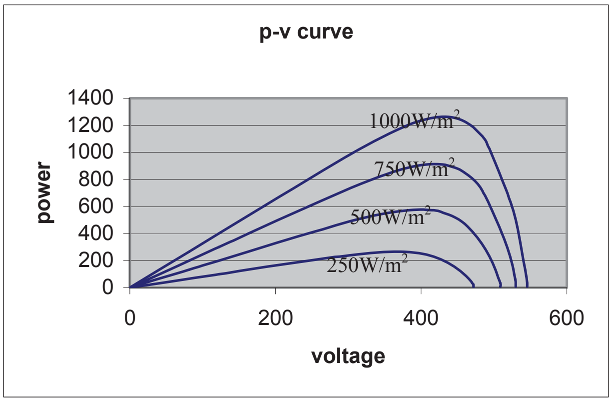

Figure 3. *p-v* curves of the PV array

In addition, there is a MPPT control circuit as a part of the PV system. The objective of the MPPT controller is to set up the DC-bus reference voltage ($V_{dc\text{-}ref}$) corresponding to the PV maximum power. The inputs of the MPPT controller are the output voltage and current of the PV panels. As mentioned before, the voltage control loop will maintain the DC-bus voltage at the reference voltage level. If the DC-bus voltage reaches the reference voltage, the PV output power will be at maximum. At the same time, the active power balance among the grid, the load and the PV panels connected to the DC-bus occurs. The active power of the loads is supplied from the grid and the PV maximum power injection. Thus, the MPPT controller is independent on the current control loop and the voltage control loop of the CC-VSI because it works outside both control loops and simply focuses on setting up the DC-bus reference voltage. The fluctuation of solar irradiation leads to the variation of the DC-bus reference voltage to obtain the PV maximum power.

IV. Fibonacci Search-Based MPPT

The MPPT controller employs the line search method [11]. This method iteratively restricts and shifts the searching range so as to obtain optimal point in the range. The direction of the shift is decided by the value of a function at two points in the range. Fig. 4 is used as an example of the process of restricting and shifting.

Fibonacci sequence, which is represented by (3) is used for setting the length of the range.

$$c_{n+2} = c_{n+1} + c_n \quad (n = 1, 2, ...)$$
$$c_1 = c_2 = 1 \tag{3}$$

The sequence is calculated as

$$c_3 = 2,\ c_4 = 3,\ c_5 = 5,\ c_6 = 8,\ c_7 = 13,\ \dots \tag{4}$$

Fig. 4 shows a given *p-v* curve of the PV panel on the interval [V_{min}, V_{max}] to search for maximum power. Two of the interior points v_1 and v_2 are selected to evaluate the function f(v) (= P). Variable v is considered as the DC-bus reference voltage and f(v) can be regarded as the PV output power. If f(v_1) < f(v_2), then the maximum point must occur in the subinterval [v_1, V_{max}]; and we replace v_1 = V_{min} and V_{max} = V_{max}, and continue the search in the new subinterval [v_1, V_{max}]. If f(v_1) > f(v_2), then the maximum point must occur in the subinterval [V_{min}, v_2]; and we replace V_{min} = V_{min} and v_2 = V_{max}, and continue the search in the new subinterval [V_{min}, v_2]. It is obvious from the figure that f(v_1) < f(v_2). Consequently, the new subinterval is shifted to [v_1, V_{max}] for the next iteration, and the new two interior points (v_2 and v_3) will be selected to evaluate the function f(v).

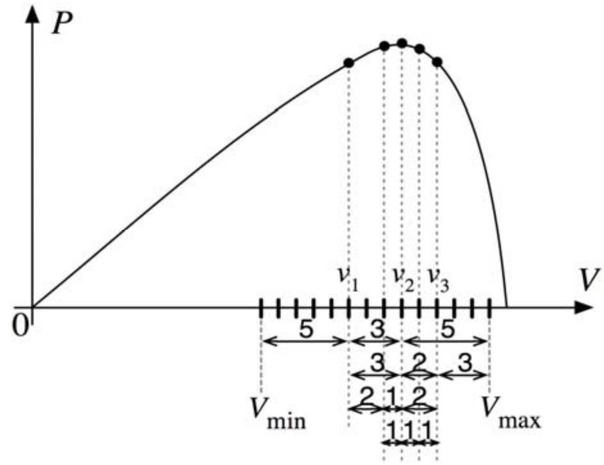

Figure 4. Searching process

From Fig. 4, the length of the range, which is determined by Fibonacci sequence in the interval [V_{min}, V_{max}] are expressed as

$$[V_{min}, v_1] = [v_2, V_{max}] = a_i = c_n,$$
$$[v_1, v_2] = b_i = c_{n-1} \tag{5}$$

The value of a_{i+1} and b_{i+1} can be decided for the next iteration as

$$a_{i+1} = c_{n-1}\ (= b_i),\ b_{i+1} = c_{n-2} \tag{6}$$

Hence, from Fig. 4, numbers on the bottom of the *p-v* curve represent Fibonacci sequence as the length of the range. Any value of n can be selected as a starting point (a_1). In this example, it is chosen to start from n = 5 and c_5 = 5. It can be seen that the search comes to the convergence when variable n becomes one. At each iteration, the length of the interval narrows according to Fibonacci sequence.

Application of the tracking process to the circuit shown in Fig. 1 will be generally as follows:

1. set $V_{dc\text{-}ref} = v_1$
2. if DC-bus voltage (V_{dc}) = v_1, due to the voltage control loop, then measure PV output power f(v_1)
3. set $V_{dc\text{-}ref} = v_2$
4. if DC-bus voltage (V_{dc}) = v_2, then measure PV output power f(v_2)
5. compare f(v_1) and f(v_2), whether f(v_1) > f(v_2) or f(v_1) < f(v_2)
6. shifting and restricting
7. return to 1 with a new $V_{dc\text{-}ref}$.

As mentioned before, the DC-bus voltage range is limited due to system stability and device insulation requirements, which is in this case in between 376V

(V_{min}) and 441V (V_{max}). Outside the limit, Fibonacci search will not be able to find the MPP.

To search the maximum power point (MPP), the Fibonacci sequence may shift to the reverse direction. The MPP may move to be outside of the search range due to a sudden change of insolation. In this case, the search range is being widening. This is realized by reversing the process in Fig. 4. The widening process is practically implemented when the range is shifted to the same direction more than M times and the Fibonacci sequence has not reached the last term c_n. For the next iteration, the value of a_{i+1} and b_{i+1} will be

$$a_{i+1} = c_{n+1}, \quad b_{i+1} = c_n \ (= a_i) \qquad (7)$$

V. Simulation Results

The system shown Fig. 1 is examined using computer simulation (PSIM®) to verify the concepts. Table 1 describes the parameter values for the system. The three-phase grid voltages contain harmonics (THD_V = 3.9%), and the mixed loads consist of single- and three-phase linear and non-linear loads (Fig. 5). The characteristics of the PV modules have been represented in Fig. 3.

As soon as the system starts, the MPPT controller iteratively limits and shifts the searching range with Fibonacci sequence as the length of the range. In this simulation, a_1 starts with n = 5 and c_5 = 5. The Fibonacci search procedure follows the rule as explained according to Fig. 4. For widening process, the value of M is 2. Fig. 6 depicts the PV output voltage, which equals to the DC-bus voltage and PV output power in steady state for insolation of 0.8kW/m^2. The system converges but oscillates around the maximum power point since the searching process still continues around n = 1. It can be seen that the DC-bus reference voltage, which equals to the output of the MPPT controller is a square wave. The voltage band of the square wave is twice of per-unit length of the range. In this simulation, the voltage per-unit length is 5V. The oscillation may lead to the problem of sub-harmonics to the power system. The voltage band can be reduced by increasing the value of n as a starting point (a_1). As a result, the voltage per-unit length decreases. However, it could increase the transient time. Fig. 6 also shows that the PV output voltage can follow the reference voltage due to the voltage control loop.

TABLE 1
Parameter Values For The System Under Study

Symbol	Description	Value
v_g	AC grid voltage, line-line, *rms*	207 V
f	AC line/grid frequency	50 Hz
L_L	Series inductor	0.92 mH
V_{dc}	DC-bus voltage (minimum)	376 V
$C_1 = C_2$	DC Capacitors, electrolytic type	4000 µF
L_{inv}	Inverter inductor	1.52 mH
f_{sw}	Target switching frequency	15.6 kHz

The average PV output voltage as well as its corresponding average maximum power matches with the insolation level according to Fig. 3. Hence, the Fibonacci-search-based MPPT controller and the voltage control loop work properly to search for the maximum PV output power and to deliver the power to the system.

Fig. 7 illustrates the load current and grid current in phase A. It is obvious that the grid current is smaller than the load current. The load active power is supplied by the grid and the maximum power extracted from the PV array. The active power balance occurs among the grid, the load and the CC-VSI along with PV panels due to the voltage control loop. Moreover, Fig. 7 shows that in spite of oscillation, the grid currents are sinusoidal, balanced and in-phase with the grid voltages due to active filtering operation. It means that the current control loop controls the harmonic and reactive power. Hence, both the current and voltage control loop operates correctly.

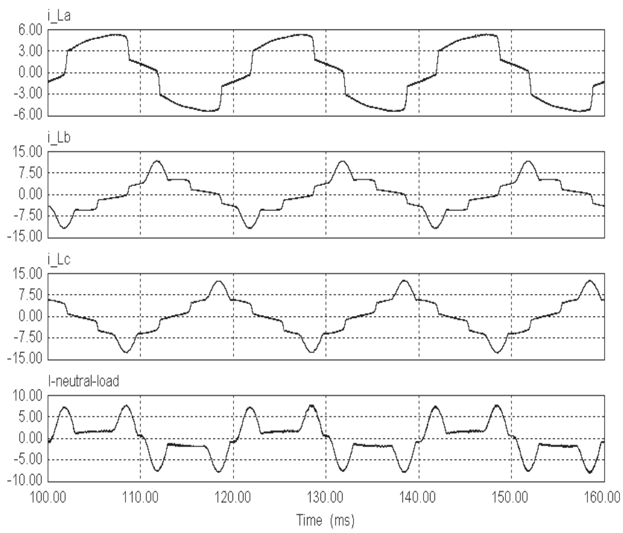

Figure 5. Mixed-load currents (phase a-b-c-neutral)

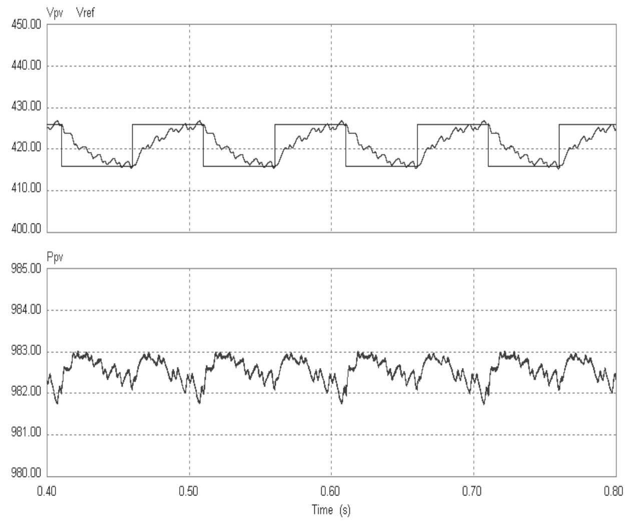

Figure 6. PV output voltage and its reference (square wave) (top); PV output power (bottom)

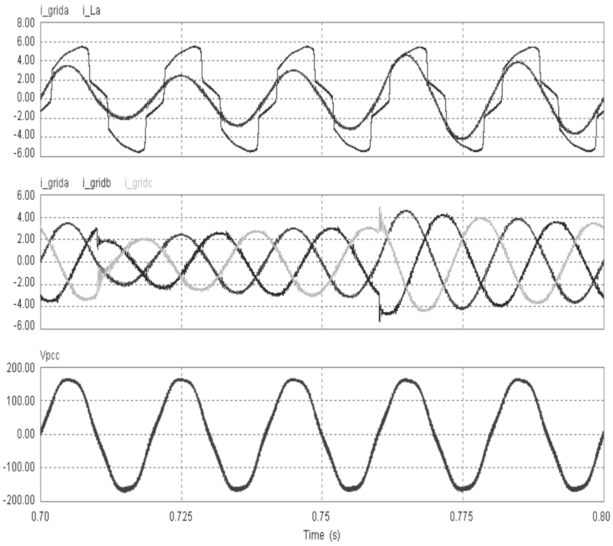

Figure 7. (top to bottom) the grid and the load currents (phase A); three-phase grid currents; the grid voltage (phase A)

When the irradiation level is below 0.3kW/m^2, the DC-bus voltage is clamped to 376V (V_{min}) due to the stability requirement. As a result, the MPPT controller would function improperly and the maximum PV output power could not be obtained. Fig. 8 demonstrates the grid and the load currents in phase A under zero insolation level. The PV panels do not supply any power and the grid totally supports the load active power. The CC-VSI simply works as a shunt active power filter. Hence, it proves that both control loops can perform independently from the MPPT controller.

Fig. 9 shows the PV output voltage and power as well as the grid current when the insolation is changed, in this case from 0.7kW/m^2 to 0.55kW/m^2. The MPPT controller responds correctly by widening the range to search another MPP. Then, the searching process continues as usual by narrowing the range to obtain the new MPP. It can be seen from Fig. 9 that the PV output voltage and power decrease. As a result, the grid current increase because the PV power delivered to the load decreases.

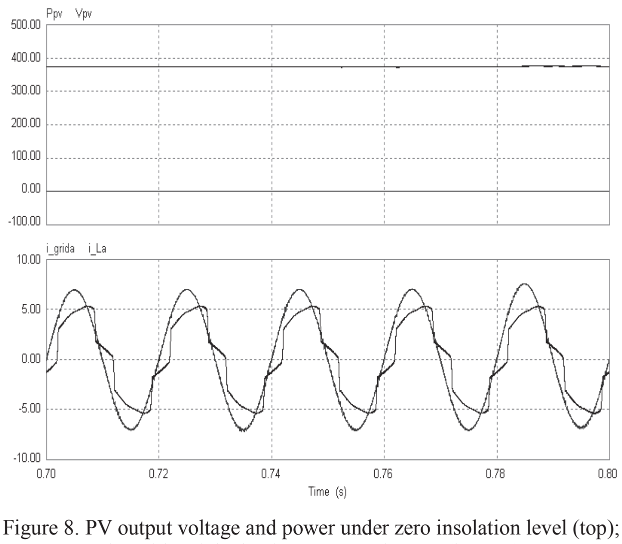

Figure 8. PV output voltage and power under zero insolation level (top); the grid and the load currents – phase A (bottom)

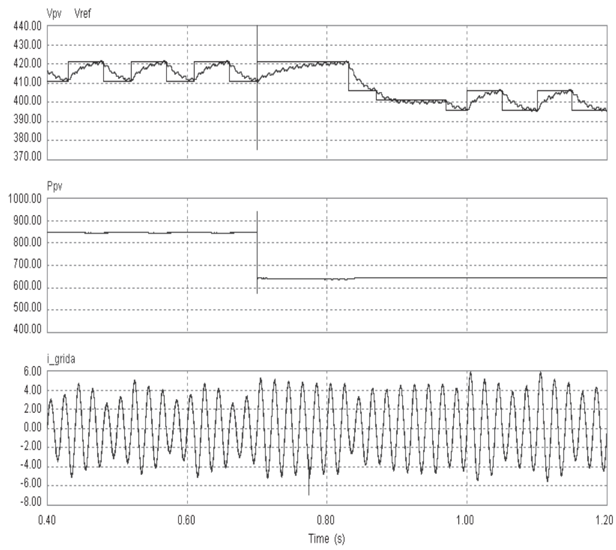

Figure 9. When the insolation is changed (0.7kW/m^2 to 0.55kW/m^2) (top to bottom): PV output voltage (and its reference); PV output power; the grid current (phase A)

VI. Conclusion

This paper describes the capability of a CC-VSI for active filtering and PV energy extraction. From simulation results, in steady state and dynamic condition, it proves that both harmonic and reactive power mitigation and PV energy extraction can be integrated effectively in one CC-VSI. The control strategy using the current control loop and the voltage control loop can handle both functions simultaneously. The system is stable and reliable. The current control loop directly shapes the grid currents to be sinusoidal and in-phase with the grid voltages, while the voltage control loop maintains the DC-bus voltage constant and regulates the active power balance among the grid, the load and the CC-VSI supported by PV panels. The load power is supplied by the grid power and the PV power. At the same time, in spite of PV output voltage oscillation, the Fibonacci-search-based MPPT controller effectively and independently searches for the PV maximum power. As a result, the energy efficiency of the system will be increased significantly.

References

[1] Borle, L., “Zero Average Current Error Control Methods for Bidirectional AC-DC Converters”, PhD Thesis, 1999, Electrical and Computer Engineering, Curtin University of Technology, Western Australia

[2] El-Habrouk, M., M.K. Darwish, and P. Mehta, “Active power filters: a review”, *Electric Power Applications, IEE Proceedings-*, 2000. **147**(5): p. 403-413.

[3] Tumbelaka, H.H., L.J. Borle, and C.V. Nayar, “Analysis of a Series Inductance Implementation on a Three-phase Shunt Active Power Filter for Various Types of Non-linear Loads”, *Australian Journal of Electrical and Electronics Engineering, Engineers Australia*, 2005. **2**(3): p. 223-232.

[4] Tumbelaka, H.H., L.J. Borle, C.V. Nayar, and S.R.Lee, “A Grid Current-controlling Shunt Active Power Filter”, *Journal of Power Electronics*, vol. 9, no. 3, 2009, p. 365-376.

[5] Chen, Y., and Smedley, K.M., “A Cost-Effective Single-State Inverter with Maximum Power Point Tracking”, *IEEE Transactions on Power Electronics*, 2004, 19(5): p. 1289-1294.

[6] Castaner, L., and Silvestre, S., "Modelling Photovoltaic System using PSpice", John Wiley & Sons, 2002.

[7] Wanzeller, M.G. et.al., "Current Control Loop for Tracking of Maximum Power Point Supplied for Photovoltaic Array", *IEEE Transactions on Instrumentation and Measurement*, 2004, 53(4): p. 1304-1310.

[8] Wu, Tsai-Fu et.al., "PV Power Injection and Active Power Filtering with Amplitude-Clamping and Amplitude-Scaling Algorithms", *IEEE Trans. on Industry Application*, 2007, **43**(3): p.731-741

[9] Grandi, G., Casadei, D., and Rossi, C., "Direct Coupling of Power Active Filters with Photovoltaic Generation System with Improved MPPT Capability", *in IEEE Power Tech Conference*, 2003. Bologna, Italy.

[10] Tumbelaka, H.H., L.J. Borle, and C.V. Nayar, "A New Approach to Stability Limit Analysis of A Shunt Active Power Filter with Mixed Non-linear Loads", *in Australasian Universities Power Engineering Conference (AUPEC)*. 2004. Brisbane, Australia: ACPE. p. ID: 121

[11] Ahmed, N.A, and Miyatake, M., "A Novel Maximum Power Point Tracking for Photovoltaic Applications under Partially Shaded Insolation Conditions", *Electric Power System Research*, 2008, **78**(5), p. 777-784.

[12] L. J. Borle, and C. V. Nayar, "Ramptime Current Control", *in Conf. Proc. 1996 IEEE Applied Power Electronics Conference (APEC'96)*, p. 828-834.

[13] L. J. Borle, and C. V. Nayar, "Zero Average Current Error Controlled Power Flow for AC-DC Power Converter", *IEEE Trans. on Power Electronics*, **10**(1): pp. 725-732. 1995.